

X-ray study of atomic correlations in $\text{Zn}_{0.5}\text{Cd}_{0.5}\text{Se}_{0.5}\text{Te}_{0.5}$ epitaxial thin films

Q. Lu, B. A. Bunker,^{*} H. Luo,[†] A. J. Kropf, K. M. Kemner,[‡] and J. K. Furdyna

Department of Physics, University of Notre Dame, Notre Dame, Indiana 46556

(Received 16 December 1996)

X-ray absorption fine-structure spectroscopy (XAFS) measurements have been performed at approximately 90 K to study the local structure of II-VI quaternary alloy $\text{Zn}_{0.5}\text{Cd}_{0.5}\text{Se}_{0.5}\text{Te}_{0.5}$. Samples were grown by molecular beam epitaxy on (100) GaAs substrates, 4° miscut towards the (111)*B* direction with a ZnTe buffer layer. The XAFS data indicate that there are more Zn-Se and Cd-Te bonds in the alloy than expected for a random arrangement. The results imply the formation of high-strain local structure and indicate that electronic pairing energies dominate over strain energy. These results are similar to the earlier observation of interlayer switching in ZnTe/CdSe superlattices. The preference of Zn-Se and Cd-Te bonding also implies a tendency to spontaneously form a composition-modulated microstructure. [S0163-1829(97)09315-6]

I. INTRODUCTION

The local structure of semiconductor alloys has long been studied both experimentally and theoretically, and is clearly closely related to the electronic and optical properties.¹⁻⁶ Although much of this work has concentrated on III-V alloys, developments in the wide-gap II-VI semiconductors have recently drawn attention due to their success in short wavelength optoelectronic applications such as blue-green laser diodes. There are to date, however, relatively few studies of the local structure of II-VI semiconductors.

One recent study⁷ suggests that entire layers of atoms interchange at ZnTe/CdSe superlattice interfaces. In this system ZnTe and CdSe are nearly lattice matched, but the atoms on both sides of the interface are still observed to switch at the interface. The formation of a high-strain structure in the superlattice suggests investigation of the alloy grown by simultaneous deposition of all the constituent elements. To explore this system, $\text{Zn}_{0.5}\text{Cd}_{0.5}\text{Se}_{0.5}\text{Te}_{0.5}$ samples were grown by molecular beam epitaxy (MBE) under similar flux ratios, growth rate, and substrate temperature as those for growing the ZnTe/CdSe superlattices. The primary motivation for the x-ray absorption fine structure (XAFS) and diffraction study of these quaternary alloys has been to understand the driving force behind the switching mechanism and to investigate structural consequences of that mechanism in a random alloy.

Artificially ordered structures, such as ZnSe/CdSe (Ref. 8) and CdTe/ZnTe (Ref. 9) layered structures, show characteristic optical properties.¹⁰⁻¹² An obvious question is whether some of these properties are related to local structure, and in particular, local ordering. The observation of atomic switching in ZnTe/CdSe superlattices indicates that atomic rearrangement may occur in II-VI compounds. Recently, spontaneous ordering has been reported in the diluted magnetic alloy $\text{Zn}_{0.5}\text{Fe}_{0.5}\text{Se}$ (Ref. 14) grown by MBE. Spontaneous short-period compositional modulation has also been discovered in $\text{ZnSe}_{1-x}\text{Te}_x$ (Ref. 15) and long-range compositional modulation has been observed in $\text{ZnSe}_{1-x}\text{Te}_x$, grown on GaAs 4° miscut towards the (111)*B* (Ref. 16) as in the present samples. Previous studies have concentrated on ternary ("pseudobinary") II-VI alloys only. Atomic rear-

angement could be much more significant in quaternary alloys than ternary alloys because of disorder on both the anion and cation sublattices.

II. SAMPLE PREPARATION AND CHARACTERIZATION

A Riber 32 R&D MBE system was used to grow the samples. For each sample, $1\ \mu\text{m}$ of GaAs was grown on top of the GaAs substrate, with a substrate temperature of 580°C , to improve the starting surface. The substrate was in the (100) direction with 4° miscut towards the (111)*B* direction. A $2\ \mu\text{m}$ ZnTe buffer layer was grown to decrease the dislocation density due to 7% lattice mismatch from GaAs to the $\text{Zn}_{0.5}\text{Cd}_{0.5}\text{Se}_{0.5}\text{Te}_{0.5}$ alloy. Finally, an epilayer of $\text{Zn}_{0.5}\text{Cd}_{0.5}\text{Se}_{0.5}\text{Te}_{0.5}$ was grown with a thickness of $2.5\ \mu\text{m}$ microns. The ZnTe and the $\text{Zn}_{0.5}\text{Cd}_{0.5}\text{Se}_{0.5}\text{Te}_{0.5}$ layers were grown with a substrate temperature of 300°C . The growth rate was kept at about 1 ML/S. A ZnTe buffer layer is nearly matched with the $\text{Zn}_{0.5}\text{Cd}_{0.5}\text{Se}_{0.5}\text{Te}_{0.5}$ alloy. X-ray rocking curve measurements of the samples show no characteristic peaks due to any constituent binary or ternary compound alloys. Transmission electron microscopy (TEM) measurements show some indications of short-range compositional modulation. Transmission electron diffraction (TED) studies, however, show no additional spots corresponding to the composition modulation.

III. XAFS MEASUREMENTS

XAFS experiments were performed at both the Se and Zn *K* edges with the x-ray polarization vector parallel and perpendicular to the sample surface; both polarizations were measured to investigate possible anisotropy in the alloy structure. The experiments were performed at approximately 90 K to reduce thermal disorder. Normally, measurements of thick samples are performed by collecting emitted x-ray fluorescence as a function of incident x-ray energy. In these single-crystal samples, however, x-ray diffraction peaks are allowed at certain energies and severely contaminate the fluorescence signal. To minimize this problem, total

electron-yield (TEY) instead of fluorescence detection has been used as the electron yield is much less sensitive to diffraction peaks.¹⁷ XAFS measurements were also performed on ZnSe and CdSe single crystals (for the Se edge), and ZnSe and ZnTe (for the Zn edge) as standards for a check on the analysis. The standards are all MBE-grown crystals.

The measurements were carried out at beam lines X11-A and X23-A2 at the National Synchrotron Light Source (NSLS). The electron beam in the storage ring had an energy of 2.5 GeV and a maximum stored current of 225 mA. Two Si (311) single crystals were used in the fixed-exit monochromator at X23A2 and in a pseudo-channel cut monochromator at X11A. The beam size at the sample was 5.0 mm wide by 0.5 mm high and 0.5 mm by 1.0 mm, respectively, for measurements with the beam polarization parallel and perpendicular to the sample surface. An ion chamber filled with nitrogen gas was used for measuring the incident beam intensity I_0 . The total electron yield is proportional to x-ray absorption by the sample and it is measured by a free-flow He gas electron yield detector. The helium gas amplifies the electron yield current by a factor of approximately 80 (Ref. 18) and also serves as a thermal exchange gas.¹⁷ Samples were set up at relatively low angles (5° – 10°) relative to the incident beam in order to spread the beam footprint over the sample. At these angles, x rays penetrate to a few thousand angstroms, which is also the approximate escape depth for

the detected secondary electrons.¹⁸ Data were collected at three different incidence angles, and three azimuthal angles at each incident angle. With such measurements, major diffraction peaks were avoided and smaller peaks distinguished from the “true” data. The remaining sharp diffraction peaks were “deglitched”¹⁹ as one of the first steps of the data analysis process.

IV. DATA ANALYSIS

The data were analyzed by using a locally modified version of the UW/NRL package. The analysis procedure is discussed in detail elsewhere.¹⁹ After removing the slowly varying background, the normalized extended XAFS data were mapped from x-ray energy space to electron wave number space (“ k space”). The normalized XAFS oscillations $\chi(k)$ for the Zn and Se edges of $\text{Zn}_{0.5}\text{Cd}_{0.5}\text{Se}_{0.5}\text{Te}_{0.5}$ are shown in Fig. 1. The $\chi(k)$ data were then Fourier transformed into real space (“ r space”) with a k^2 weighting and k -space ranges of 2.95 – 11.35 \AA^{-1} for the Zn edge and 3.05 – 11.55 \AA^{-1} for the Se edge. The Fourier-transformed “ r -space” data are shown in Fig. 2. To isolate the nearest-neighbor information, data were inverse Fourier transformed with window width of 2.0 \AA for the Zn edge and 1.8 \AA for the Se edge. These data were then fit to reference data from the standards ZnSe, ZnTe, CdSe, and CdTe. The experimental single-shell data and the resulting fits are shown in Fig. 3,

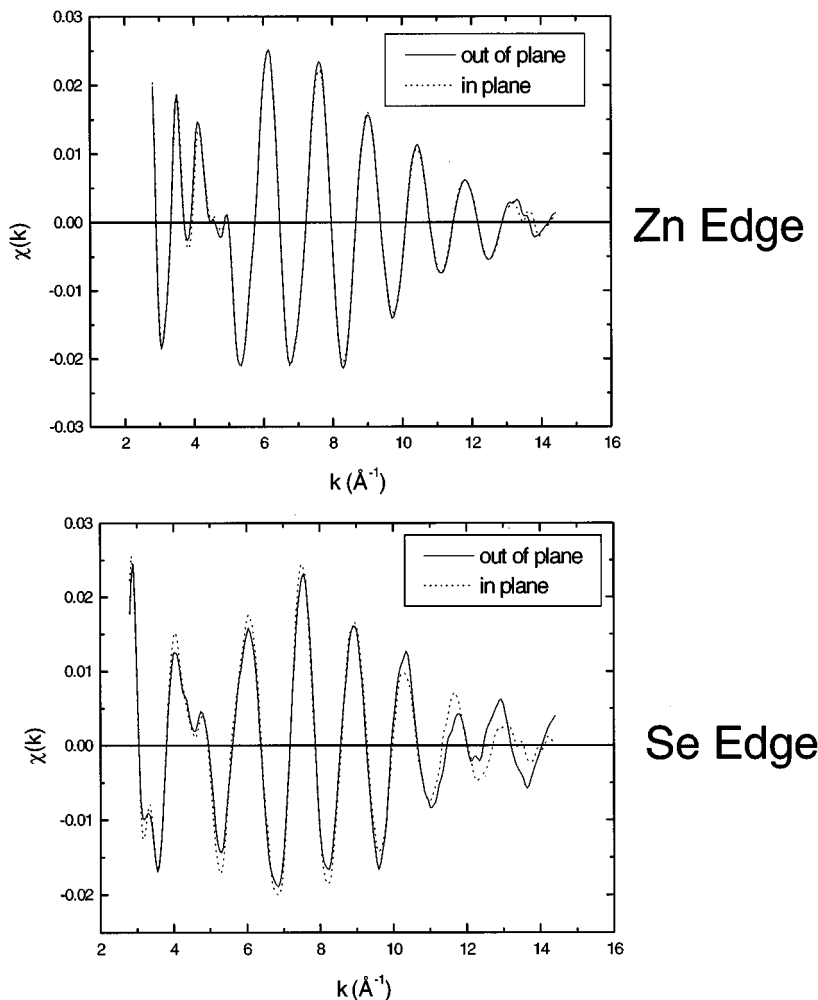
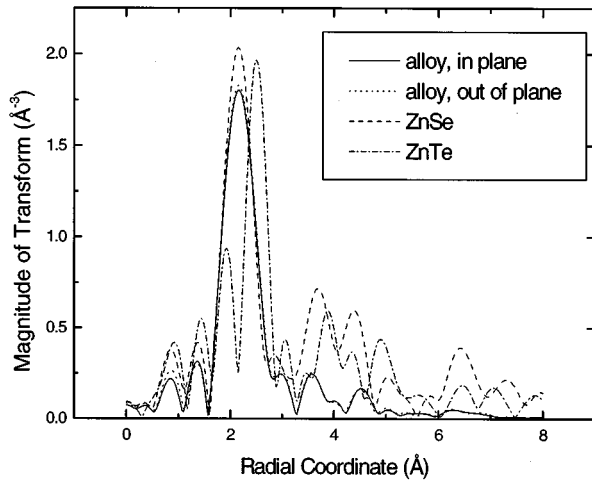
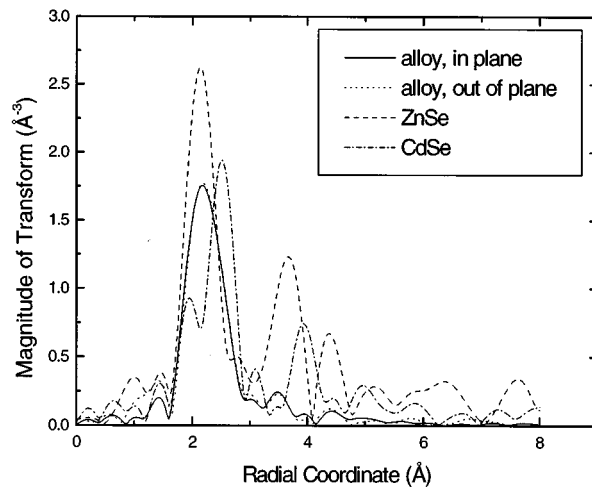


FIG. 1. (a) Normalized EXAFS oscillations, $\chi(k)$, corresponding to the (a) Zn and (b) Se K edges of $\text{Zn}_{0.5}\text{Cd}_{0.5}\text{Se}_{0.5}\text{Te}_{0.5}$ measured at approximately 85 K. The solid lines denote measurements with the x-ray polarization perpendicular to the sample surface while the dotted lines denote polarization parallel to the surface (e.g., parallel to the growth direction).



Zn Edge



Se Edge

FIG. 2. Magnitude of the k -weighted Fourier transform of (a) Zn and (b) Se K -edge $k^2\chi(k)$ data for the alloy (both polarizations) and standards.

while the resulting structural parameters are summarized in Table I.

V. RESULTS AND DISCUSSION

In Fig. 2, where the Zn edge r -space data are shown, the $\text{Zn}_{0.5}\text{Cd}_{0.5}\text{Se}_{0.5}\text{Te}_{0.5}$ r -space XAFS spectrum (which is related to a radial distribution function) of the alloy is seen to be more similar to ZnSe than to ZnTe. A similar effect is seen for the Se edge, where the $\text{Zn}_{0.5}\text{Cd}_{0.5}\text{Se}_{0.5}\text{Te}_{0.5}$ shape is much closer to ZnSe than to CdSe. These qualitative observations suggest that there are more ZnSe bonds than ZnTe bonds and more ZnSe bonds than CdSe bonds.

Quantitative results are obtained from the fits, which are summarized in Table I. These results agree with the qualitative conclusions, showing there are more Se than Te atoms around Zn atoms, and more Zn than Cd atoms around the Se atoms. Note that the results from the Zn and Se edges are independent, but are consistent with each other within the experimental uncertainties. Unfortunately, the K -edge energies for both Cd and Te are too high (and the L -edge energies too closely spaced) to obtain good quality data with the experimental facilities used here, so direct measurements of the Cd-Te coordination were not possible. However, note that the preference of Zn-Se bonds and a deficit of Cd-Se and Zn-Te bonds all imply a preference for Cd-Te bonds.

The preference of Zn-Se and Cd-Te bonds is consistent with the result of the XAFS studies of interfaces in ZnTe/CdSe superlattices. A recent study⁷ suggests that CdSe/ZnTe superlattices exhibit a switching of nearly entire planes of atoms at the interfaces between the two materials. This work demonstrates that the switching mechanism could be driven by the relative pairing energies (or pair potentials) of Zn-Se, Zn-Te, Cd-Se, and Cd-Te at the cost of increased strain energy.

The competition of “pairing” bond formation and strain energies are also expected to be important in the random alloy. The strain energy is highly dependent on the size of the constituent atoms. To minimize the total strain in the system, one would expect that Zn-Te and Cd-Se bonds be preferred, which is opposite of the experimental results here. An explanation lies in the differences in bond formation of binary compounds in the alloys. The bond-formation energy is simply the reduction in total energy in forming a pair bond.²⁰ The sum of bonding energies for ZnSe and CdTe is about 0.26 eV higher than that of ZnTe and CdSe. This inequality suggests that the ZnSe and the CdTe pairs have a higher tendency to form than ZnTe and CdSe pairs. This is also supported qualitatively by the fact that ZnSe has much higher melting point than the other binary compounds in the alloy, and the sum of the band gap of ZnSe and CdTe is 0.20 eV higher than that sum of ZnTe and CdSe. From our mea-

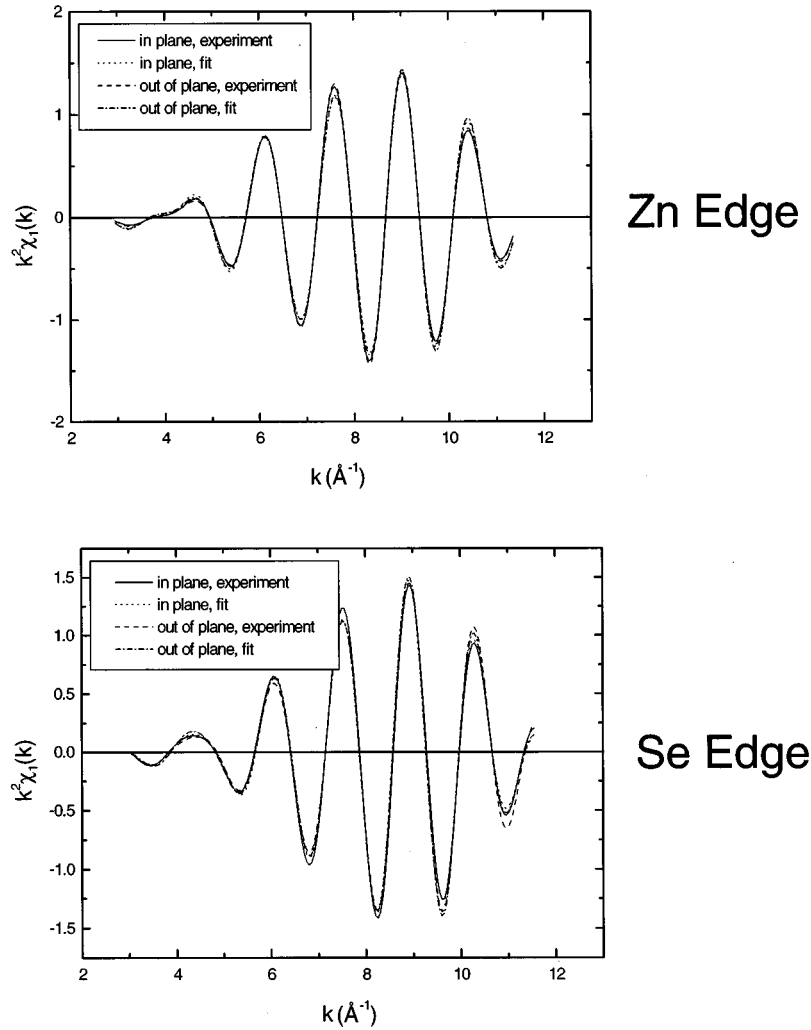


FIG. 3. Least-square fits and experimental first-shell data for (a) Zn and (b) Se K -edge k^2 -weighted single-shell χ_1 data, for the Zn $_{0.5}\text{Cd}_{0.5}\text{Se}_{0.5}\text{Te}_{0.5}$ alloy in both polarizations.

measurements, the bonding energies apparently favor the formation of ZnSe and CdTe, which overcome minimization of strain energy.

Similar XAFS studies have been performed on the III-V quaternary alloy $\text{Ga}_x\text{In}_{1-x}\text{As}_y\text{Sb}_{1-y}$.²¹ The III-V quaternary results showed the Ga-As pairs were preferred over In-As pairs. These results are similar to our II-VI findings and also imply the formation of high-strain microstructure. A major difference between the previous III-V studies and our present work is in sample preparation. The previous III-V study was performed on polycrystalline powder samples that

have a relatively large surface area, while these current measurements were performed on single-crystal epitaxial films. This can be important for some cases because surface and interfaces may not have the same boundaries to phase segregation as the bulk single crystals. Despite these differences, the results of the two studies are in agreement.

A further corroboration of these results is seen in dark-field TEM images¹³ of the $\text{Zn}_x\text{Cd}_{1-x}\text{Se}_y\text{Te}_{1-y}$ alloy, which show some indications of short-range composition variations. Since ZnSe and CdTe bonds are preferred and the “average” alloy has equal numbers of Zn, Se, Cd, and Te

TABLE I. Structural parameters of $\text{Zn}_{0.5}\text{Cd}_{0.5}\text{Se}_{0.5}\text{Te}_{0.5}$ as obtained from XAFS measurements.

K edge	Polarization	Bonds	Correlation number	Nearest-neighbor distance (\AA)
Zn	Parallel	Zn-Se	$3.28^{+0.3}_{-0.6}$	2.47 ± 0.01
		Zn-Te	$0.72^{+0.6}_{-0.3}$	2.58 ± 0.04
	Perpendicular	Zn-Se	$3.24^{+0.3}_{-0.6}$	2.47 ± 0.01
		Zn-Te	$0.76^{+0.6}_{-0.3}$	2.60 ± 0.04
Se	Parallel	Se-Zn	2.60 ± 0.4	2.46 ± 0.01
		Se-Cd	1.40 ± 0.4	2.63 ± 0.02
	Perpendicular	Se-Zn	2.69 ± 0.3	2.46 ± 0.01
		Se-Cd	1.31 ± 0.3	2.62 ± 0.02

atoms, the alloys must be segregated into ZnSe-rich and CdTe-rich regions. The XAFS data shown in Fig. 1 show no change in coordination between the parallel and perpendicular orientations, which is consistent with the lack of long-range order.

In summary, XAFS measurements of epitaxial thin films of the II-VI alloy $\text{Zn}_{0.5}\text{Cd}_{0.5}\text{Se}_{0.5}\text{Te}_{0.5}$ clearly show that there are more Zn-Se and Cd-Te bonds in the alloy than expected for a random alloy. There is no statistically significant difference in coordination parallel and perpendicular to the growth direction. The observed preference is also consistent with the previously studied atomic-layer switching at the interfaces of ZnTe/CdSe superlattice. The XAFS results would imply some sort of short-range composition modulation, and this is seen in dark-field TEM images. There is no

evidence for long-range ordering of either local structure or the composition fluctuations, however.

ACKNOWLEDGMENTS

We thank Kathie Newman for useful discussions and comments on the manuscript. The X11-A beamline is supported in part by the U.S. Department of Energy, Division of Materials Sciences, Office of Basic Energy Sciences. The X23-A2 beamline is supported in part by the National Institute of Standards and Technology. Two of us (H.L. and J.K.F.) acknowledge the support of NSF/MRG Grant DMR 9221390. K. M. Kemner received financial support from the Naval Research Lab and the National Research Council.

*To whom correspondence should be addressed. Electronic address: bunker.1@nd.edu.

†Present address: Department of Physics and Astronomy, State University of New York at Buffalo, Buffalo, NY 14 260.

‡Present address: Argonne National Laboratory, Argonne, IL 60 439.

¹S. H. Wei and A. Zunger, Phys. Rev. B **49**, 14 337 (1994).

²K. A. Mader and A. Zunger, Phys. Rev. B **51**, 10 462 (1995).

³S. N. Ekpenuma, C. W. Myles, and J. R. Gregg, Phys. Rev. B **41**, 3582 (1990).

⁴Y. Cai and M. F. Thorpe, Phys. Rev. B **46**, 15 872 (1992).

⁵Y. Cai and M. F. Thorpe, Phys. Rev. B **46**, 15 879 (1992).

⁶N. Mousseau and M. F. Thorpe, Phys. Rev. B **46**, 15 887 (1992).

⁷K. M. Kemner, B. A. Bunker, H. Luo, N. Samarth, J. K. Furdyna, M. R. Weidmann, and K. E. Newman, Phys. Rev. B **46**, R7272 (1992); and **50**, 14 327 (1994).

⁸H. Luo, N. Samarth, A. Yin, A. Pareek, M. Dobrowolska, J. K. Furdyna, K. Mahalingam, M. Otsuka, F. C. Peiris, and J. R. Buschert, J. Electron. Mater. **22**, 467 (1993).

⁹J. Li, L. He, W. Shan, X. Cheng, and S. Yuan, J. Cryst. Growth **111**, 736 (1991).

¹⁰H. Jeon, J. Ding, A. B. Nurmikko, H. Luo, N. Samarth, J. K. Furdyna, W. A. Bonner, and R. E. Nahory, Appl. Phys. Lett. **57**, 2413 (1990).

¹¹M. A. Haase, J. Qiu, J. M. DePuydt, and H. Cheng, Appl. Phys. Lett. **59**, 1272 (1991).

¹²Z. Yu, J. Ren, B. Sneed, K. A. Bowers, K. J. Gossett, C. Boney, Y. Lansari, J. W. Cook, Jr., J. F. Schetzina, G. H. Hua, and N. Otsuka, Appl. Phys. Lett. **61**, 1266 (1992).

¹³G. H. Hua (unpublished).

¹⁴K. Park, L. Salamanca-Riba, and B. T. Jonker, Appl. Phys. Lett. **61**, 2302 (1992).

¹⁵H. Luo, N. Samarth, S. W. Short, S. H. Xin, J. K. Furdyna, P. Ahrenkiel, M. H. Bode, and M. M. Al-Jassim, J. Vac. Sci. Technol. B **12**, 1140 (1994).

¹⁶S. P. Ahrenkiel, S. H. Xin, P. M. Reimer, J. J. Berry, H. Luo, S. Short, M. Bode, M. Al-Jassim, J. R. Buschert, and J. K. Furdyna, Phys. Rev. Lett. **75**, 1586 (1995).

¹⁷K. M. Kemner, A. J. Kropf, and B. A. Bunker, Rev. Sci. Instrum. **65**, 3667 (1994).

¹⁸W. T. Elam, J. P. Kirkland, R. A. Neiser, and P. W. Wolf, Phys. Rev. B **38**, 26 (1988).

¹⁹D. Sayers and B. Bunker, in *X-Ray Absorption: Principles, Applications, Techniques of EXAFS, SEXAFS, and XANES*, edited by D. C. Konigsberger and R. Prins (Wiley, New York, 1987), Chap. 6.

²⁰W. A. Harrison, in *Electronic Structure and the Properties of Solids* (Dover, New York, 1989).

²¹S. M. Islam and B. A. Bunker, Phys. Lett. A **156**, 247 (1991).